ELSEVIER

Neurobiology of Disease

www.elsevier.com/locate/ynbdi
Neurobiology of Disease 28 (2007) 237–250

Minocycline, a possible neuroprotective agent in Leber's hereditary optic neuropathy (LHON): Studies of cybrid cells bearing 11778 mutation

Mohammad Fahad Haroon,[a,*] Ambrin Fatima,[a] Susanne Schöler,[b] Anne Gieseler,[a] Thomas F.W. Horn,[a] Elmar Kirches,[b] Gerald Wolf,[a] and Peter Kreutzmann[a,*]

[a]*Institute of Medical Neurobiology, Otto-von-Guericke University of Magdeburg, Leipziger Strasse 44, D-39120 Magdeburg, Germany*
[b]*Institute of Neuropathology, Otto-von-Guericke University of Magdeburg, D-39120 Magdeburg, Germany*

Received 19 March 2007; revised 25 June 2007; accepted 10 July 2007
Available online 28 July 2007

Leber's hereditary optic neuropathy (LHON) is a retinal neurodegenerative disorder caused by mitochondrial DNA point mutations. Complex I of the respiratory chain affected by the mutation results in a decrease in ATP and an increase of reactive oxygen species production. Evaluating the efficacy of minocycline in LHON, the drug increased the survival of cybrid cells in contrast to the parental cells after thapsigargin-induced calcium overload. Similar protection was observed by treatment with cyclosporine A, a blocker of the mitochondrial permeability transition pore (mPTP). Ratiometric Ca^{2+} imaging reveals that acetylcholine/thapsigargin triggered elevation of the cytosolic calcium concentration is alleviated by minocycline and cyclosporine A. The mitochondrial membrane potential of LHON cybrids was significantly conserved and the active-caspase-3/procaspase-3 ratio was decreased in both treatments. Our observations show that minocycline inhibits permeability transition induced by thapsigargin in addition to its antioxidant effects. In relation with its high safety profile, these results would suggest minocycline as a promising neuroprotective agent in LHON.

Keywords: Permeability transition; Mitochondria; Thapsigargin; Calcium imaging; Complex I; Apoptosis; Minocycline; Leber's hereditary optic neuropathy; LHON

Introduction

Leber's hereditary optic neuropathy (LHON) is characterized by an acute or subacute, bilateral central vision loss due to degeneration of retinal ganglion cells and the optic nerve. Until now, only a handful of definitively proven pathogenic mutations (so called primary LHON mutations) have been established, all of which lead to amino acid exchanges in some subunits of the NADH:ubiquinone–oxidoreductase (complex I) of the respiratory chain. Only three of these mutations located at base pairs 3460, 11778, and 14484 in the mitochondrial genome have been observed in more than a few families worldwide. The cybrid technology lends itself to study this disease as the degenerating optic nerve is generally not accessible until the death of the patient and by that time the extent of the ailment is to its maximum with degeneration to full extent. Also the model provides a valuable tool to assess and correlate to other diseases a possibly similar mitochondrial pathomechanism e.g. Parkinson's, Alzheimer's, and Huntington's disease.

The amino acid sequence changes of the mitochondrial complex I affect its functioning and lead to a decrease in mitochondrial ATP synthesis, as shown in cybrid cell cultures (Baracca et al., 2005). This declined oxidative phosphorylation can lead to even further decreased ATP levels in cells under conditions blocking non-oxidative ATP generation (Zanna et al., 2005). ATP deficiency is thus thought to be one possible explanation of ganglion cell degeneration *in vivo* because the unmyelinated retinal axon sections theoretically have an extraordinary high energy demand, which is reflected by enhanced cytochrome c oxidase activity (Carelli et al., 2004). On the other hand, oxidative stress by increased superoxide production may play a role since complex I is a superoxide generating site of the respiratory chain and, accordingly, ROS (reactive oxygen species) sensitive fluorescent dyes detected higher oxidative stress in mutant cybrid cells (Wong et al., 2002). In addition calcium overload in the cytoplasm (e.g. following

Abbreviations: LHON, Leber's hereditary optic neuropathy; mPTP, mitochondrial permeability transition pore; ROS, reactive oxygen species; CsA, cyclosporin A; AcCh, acetylcholine; TG, thapsigargin; TMRM, tetramethyl rhodamine methyl ester; MC, minocycline; MTT, 3-[4,5-dimethylthiazol-2-yl]-2,5-diphenyl tetrazolium bromide; aC3/pC3, active-caspase-3/procaspase-3; DFF, difluorofluorescein; rpm, rotations per minute.

* Corresponding authors. Fax: +49 391 6714365.
E-mail addresses: Fahad.Haroon@medizin.uni-magdeburg.de (M.F. Haroon), Peter.Kreutzmann@medizin.uni-magdeburg.de (P. Kreutzmann).

Available online on ScienceDirect (www.sciencedirect.com).

0969-9961/$ - see front matter © 2007 Elsevier Inc. All rights reserved.
doi:10.1016/j.nbd.2007.07.021

overexcitation) and the mitochondrial matrix may enhance the oxidative stress and thereby increase the probability of opening of mitochondrial permeability transition pore (mPTP) followed by the release of cytochrome c and apoptosis (Kantrow and Piantadosi, 1997). The declining defensive strength of cellular protection with age and environmentally induced oxidative stress can further provoke the onset of the disease (Kasapoglu and Ozben, 2001; Head et al., 2002). Oxidative stress in LHON cybrids was previously discussed (Floreani et al., 2005).

There has been extensive research on the biochemical consequence of the mutations in LHON disorder and elucidation of pathological pathways of the disease (Carelli et al., 1997, 1999; Brown, 1999; Howell, 2003). Not much work however has been put into the investigation for a treatment or pharmacological intervention of the disease. Antioxidants and mPTP blockers can possibly be effective in such pathology. Minocycline, a semi-synthetic second generation tetracycline, has been shown to be, apart from its antimicrobial actions, effective in various models of neurodegenerative disorders like Parkinson's and Huntington's disease, spinal cord injury, and amyotrophic lateral sclerosis (Yong et al., 2004). Currently, minocycline is under clinical investigation for stroke and spinal cord injury (Fehlings and Baptiste, 2005). Although there are contradictory or inconclusive results, minocycline still remains one of the most interesting potential neuropharmaceuticals for clinical trials because of its broad spectrum of protective actions and good tolerability. Beneficial effects of minocycline in LHON have not been reported so far. Here we study in a cybrid cell model of LHON disorder the effects of minocycline on parameters of mitochondrially mediated cellular degeneration induced by thapsigargin (TG).

Methods

Chemicals and cell lines

Minocycline, MTT (3-[4,5-dimethylthiazol-2-yl]-2,5-diphenyl tetrazolium bromide), Fura PE3-AM, Dulbecco's modified Eagle's medium (DMEM), Acetylcholine (AcCh), and uridine were purchased from Sigma and cyclosporine A (CsA) from Alexis Biochemicals. TG, Mitotracker green, TMRM (tetramethyl rhodamine methyl ester), and H_2DFFDA (5-(and-6)-carboxy-2′,7′-difluorodihydrofluorescein diacetate) were obtained from Molecular Probes. Sodium pyruvate, fetal calf serum, penicillin/streptomycin and L-glutamine were purchased from PAA Laboratories. Caspase-3 antibody H-277:(sc-7148) used for Western blotting was from Santa Cruz Biotechnology Inc. and the active-caspase-3 antibody from Epitomics. Protease inhibitor cocktail (Complete mini) and "ATP Bioluminescence Assay Kit CLS II" were acquired from Roche. NT2 human teratoma derived cell lines were used as the parental controls and were obtained from ATCC (American Type Culture Collection). Cybrid cells with a G to A point mutation at the 11778 base pair of the mitochondrial DNA (which affects the amino acid sequencing of the ND4 subunit of complex I in the respiratory chain) were used as the LHON disorder model. In these cybrid (cytoplasmic hybrid) tumor cell lines, the mitochondrial DNA had been selectively replaced by that of one LHON patient carrying the appropriate mutation. For this purpose, the mtDNA of the tumor cell line was first removed by prolonged sublethal ethidium bromide treatment and the resulting rho zero cells were then fused with enucleated patient fibroblasts. While the method was initially introduced by Micheal King and Guiseppe Attardi in 1989 using osteosarcoma cells, the cybrids analyzed in this study were prepared from the NT2/D1 teratoma cell line (Wong et al., 2002). This cell line was a generous gift from G. A. Cortopassi (Department of Molecular Biosciences, University of California Davis, Davis, CA 95616, USA) (5). All cells were stored in a cryogenic solution under liquid nitrogen.

Cell culturing

NT2/D1 (NT2) cells and 11778-1 LHON cybrid cells (LHON) (Schoeler et al., 2007) were cultivated in DMEM (high glucose, D 5648-Sigma) with 110 mg/l of sodium pyruvate, 1.5 g/l $NaHCO_3$, 100 ml/l fetal calf serum, 50 mg/l uridine, 10 ml/l L-glutamine, and penicillin/streptomycin. For propagation, cells were trypsinized, resuspended in the culture medium and plated at the required density (approximately 10^5 cells per ml) in incubating flasks or onto sterile glass coverslips.

Cell survival assay

Colorimetric MTT reduction assay was used to assess cell viability. LHON cybrid cells and NT2 cells were grown in a 24 well plate for 24 h (0.5 ml per well) before a stimulus with 1 μM TG was given for a duration of 12 h. Treated groups ($n=12$ in each case) were incubated with the drug 30 min prior to the stimulus. After incubation the medium was replaced by 0.5 ml of 1 mg/ml MTT solution in PBS for 1 h. The formazan formed by the mitochondria of viable cells was then dissolved in DMSO (dimethyl sulfoxide) and the optical density of the solution measured on an ELISA plate reader at 570 nm. Cultures were tested for the survival of cells with different concentrations of minocycline (50, 75, 100, 125, 150, and 200 μM) and CsA (1, 2, 3, and 5 μM) against TG-induced calcium overload and resulting cell death. The percentage of survival was calculated by taking the arithmetic mean of control values (survival of cells without treatment) as reference.

ATP measurements

LHON cybrids and NT2 cells were treated with 1 μM TG for 0.5, 1, or 2 h and without or with prior adding of 100 μM minocycline. Afterwards the cells were trypsinized and spun down at 1000×*g* for 5 min. The supernatant was discarded and the pellet resuspended in PBS. After a centrifugation at 1000×*g* for 2 min the supernatant was replaced by boiling ATP measurement buffer (100 mM Tris, 4 mM EDTA, pH 7.75) and incubated for 2 min at 100 °C. The samples were centrifuged at 1000×*g* for 1 min and the supernatant was transferred to a fresh tube and mixed with luciferase reagent (ATP assay Kit CLS II, Roche). For the measurement of luminescence intensity a TD-20/20 luminometer was used. The luminescence was calibrated with a standard ATP curve and regression was applied to get the ATP concentrations from the samples. These values were then adjusted to the protein level of the samples. The total level of protein was determined by using the bicinchoninic acid assay (BCA protein assay kit, Pierce).

Ca^{2+} imaging

Cells were cultured on sterile coverslips and visualized for live cell imaging 32–48 h later. Fura PE3-AM was used as fluorescent ratiometric calcium indicator. Microscopy was done with Meta Fluor software on a Zeiss Axiovert 100M Pascal confocal microscope with

Visitron Systems GmbH setup. All cells were incubated with the dye at a concentration of 5 μM for 30 min and afterwards washed with HBSS (HEPES buffer salt solution: NaCl 8.006 g/l, KCl 373 mg/l, $MgCl_2$ 0.182 mg/l, HEPES 4.76 g/l, glucose 991 mg/l, KH_2PO_4 81 mg/l, K_2HPO_4 0.01 mg/l, $NaHCO_3$ 840 mg/l, and $CaCl_2$ 205 mg/l, adjusted to pH 7.4) once to drain away excess dye. The coverslips were then placed in a fixed chamber and mounted on a thermostatic metallic grid (maintained at 37 °C) on the microscope and perfused with HBSS at 37 °C with or without the drug investigated. For evaluating the effects of minocycline and CsA the cultures were incubated with the respective drug for 30 min prior to the commencement of the imaging. At the beginning of the experiment, buffer was perfused through the culture for 3 min to get a stable baseline after which the experimental recording was started. The experimental workflow is schemed in Fig. 3A. In these experiments acetylcholine (AcCh) was used to induce an acute calcium release after which TG at a concentration of 1 μM was perfused to completely and irreversibly inhibit the reuptake of calcium back to the endoplasmic stores. The change in the cellular calcium was measured by the ratio of the two fluorescence intensities at 340 nm and 380 nm, which corresponds to the calcium bound and the native form of the dye.

Mitochondrial depolarization

Cells were cultured on poly-D-lysine coated coverslips for 24 h and mitochondrial depolarizing experiments were conducted in cell culture medium, which was deficient in serum. TMRM (100 nM) was used to assess the mitochondrial depolarization and Mitotracker green (160 nM) for simultaneously visualizing the total population of mitochondria. After 8 h of incubation with 1 μM TG and without or with 100 μM minocycline or 3 μM CsA ($n=6$ in each), the coverslips were incubated with Mitotracker green and TMRM for 30 min and view fields were selected randomly for taking pictures with the confocal microscope. Cells from different coverslips were counted for those stained with Mitotracker green (total number of cells) and for those that were additionally stained with TMRM (cells with conserved mitochondrial membrane potential). From each of the six cultures from every treatment five pictures were taken and pooled for analysis. Percentage of cells with intact mitochondrial membrane potential was calculated by dividing the number of TMRM stained cells by the total number of cells stained with Mitotracker green.

Western blotting

The ratio of active-caspase-3 to procaspase-3 (aC3/pC3) was calculated by analysis of the Western blots of LHON cybrid cells and the NT2 cell line subjected to TG. The time point of sample collection was 8 h after incubation with 1 μM TG and with or without treatments. For statistical analysis 5 samples per group ($n=5$) were evaluated with the exception of NT2 cells treated with minocycline ($n=4$) and CsA ($n=3$). The cells were scrapped and then spun down at 1500 rpm for 5 min. Pellets were resuspended in 0.05 M sodium phosphate solution containing protease inhibitor cocktail and transferred to an Eppendorf tube and spun again. After homogenization of the pellets with a Teflon tip homogenizer and centrifugation at 14,000 rpm for 5 min the obtained supernatants were taken for analysis.

Electrophoresis was done on gradient acrylamide gel (5–20%), casted in a Hoeffer gel caster with the same quantity of protein sample loaded in each well. The blots were developed using Western blotting detection reagents and Hyperfilm (Amersham). The detected two bands correlate to 19 and 17 kDa and are probably cleaved (active) forms of procaspase-3 proteins (Kim et al., 2000; Schauser and Larsson, 2005). Band intensities of the blots obtained with Quantity one (1D analysis software from BioRad) were subjected to calculation of aC3/pC3 ratio. The ratios of normal untreated groups were normalized to a value of 1.

DFF imaging

H_2DFFDA is a photostable congener of the widely used intracellular ROS detecting dye DCF which fluoresces upon oxidation (Jakubowski and Bartosz, 2000). Experiments were performed on cells cultured on coverslips, incubated with the dye for 1 h and the respective drugs for 30 min and finally mounted onto the confocal microscope in a thermostatic chamber. The medium was replaced with 990 μl of modified Locke's solution (NaCl 7.58 g/l, KCl 300 mg/l, $CaCl_2$ 240 mg/l, $MgSO_4$ 240 mg/l, $NaHCO_3$ 340 mg/l, HEPES 2.42 g/l, glucose 1.82 g/l, adjusted to pH 7.3) without and with different concentrations of minocycline (10 μM, 25 μM, 50 μM, and 100 μM), 3 μM CsA, and 100 μM vitamin C. Fluorescence (excitation at 488 nm and emission at 530 nm) was measured in live cells using a Zeiss Axiovert 100M Pascal confocal microscope for 10 min. Experimental settings including the pinhole diameter, intensity of the laser, and the detector gain were kept uniform in all the experiments performed. The first 100 s of the measurement was used to obtain a steady baseline after which 10 μl of 10 mM H_2O_2 solution (final concentration of 100 μM) in modified Locke's solution was injected into the monitored culture.

Statistical analysis

All results are expressed as mean ± S.E.M. One way ANOVA followed by Dunnett's t test was performed to assess the differences between and within the treatment groups in all experiments where more than two groups were planned for comparison. For the results obtained by calcium imaging the fluorescence values were collapsed at every 100-second time point after the withdrawal of calcium stimulus. For this experiment, a two-way ANOVA was done to assess bi-factorial treatment × time effect. A p value of F statistics less than 0.05 indicates that at least one pair of the treatment groups differed significantly in the two-way ANOVA. Bonferroni's multiple comparison test was applied to test exactly which pair(s) of treatment significantly differed. Student's t test was used to evaluate whether TG induced a significant difference in the aC3/pC3 ratio between the two cell lines. All statistical tests were done by using GraphPad Prism 4 (GraphPad Softwares).

Results

Minocycline and CsA protect against thapsigargin (TG)-induced cell death

Cell surviving studies on LHON 11778 cells applying different concentrations of TG resulted in a median lethal dose (LD_{50}) of 1.0 μM (data not shown). This amount of TG significantly decreased the percentage of survival in both cell lines (in Fig. 1A: NT2 71.7 ± 0.67%, $p<0.05$ and LHON cybrid 49.5 ± 1.96%,

$p<0.05$; in Fig. 1B: NT2 69.2±0.73%, $p<0.05$ and LHON cybrid 53.7±2.68%, $p<0.05$). Difference in the survival rate of LHON verses NT2 cells treated with TG was also significant. The concentration response curve in Fig. 1A shows for LHON cybrid cells that treatment with minocycline at concentrations of 100 and 125 μM prevents cell death as indicated by a higher rate of survival. A minimum effective dose of minocycline in the LHON cybrid cells was found to be 100 μM (78.8±1.72%, $p<0.05$). At higher doses (150 and 200 μM) there was manifestation of toxic effects of minocycline because the percentage of survival significantly decreases to 53.9±3.3% and 48.3±2.3%, respectively. In the parental cell lines however, the protective effect of minocycline was not observed at any concentration. Toxic effect of minocycline at concentrations of 150 and 200 μM, as seen in the cybrid cells, was observed in the NT2 cell line as well. Concentration response curve of CsA in the two cell lines (Fig. 1B) showed that there is no significant increase in cell survival at any concentration in the NT2 cells whereas the minimum effective dose in the LHON cybrid cells was 2 μM (68.7±0.95%, $p<0.05$). In addition, 3 μM CsA (74.78±1.31%) shows a significantly higher protection than 2 μM CsA solution in cybrid cells.

Thapsigargin (TG) treatment decreases ATP levels in LHON cybrids

The ATP levels (per mg of protein) of LHON cybrids, initially, decreased significantly (after 1 h) but returned to the original value after 2 h of TG treatment (Fig. 2). In contrast the ATP levels of

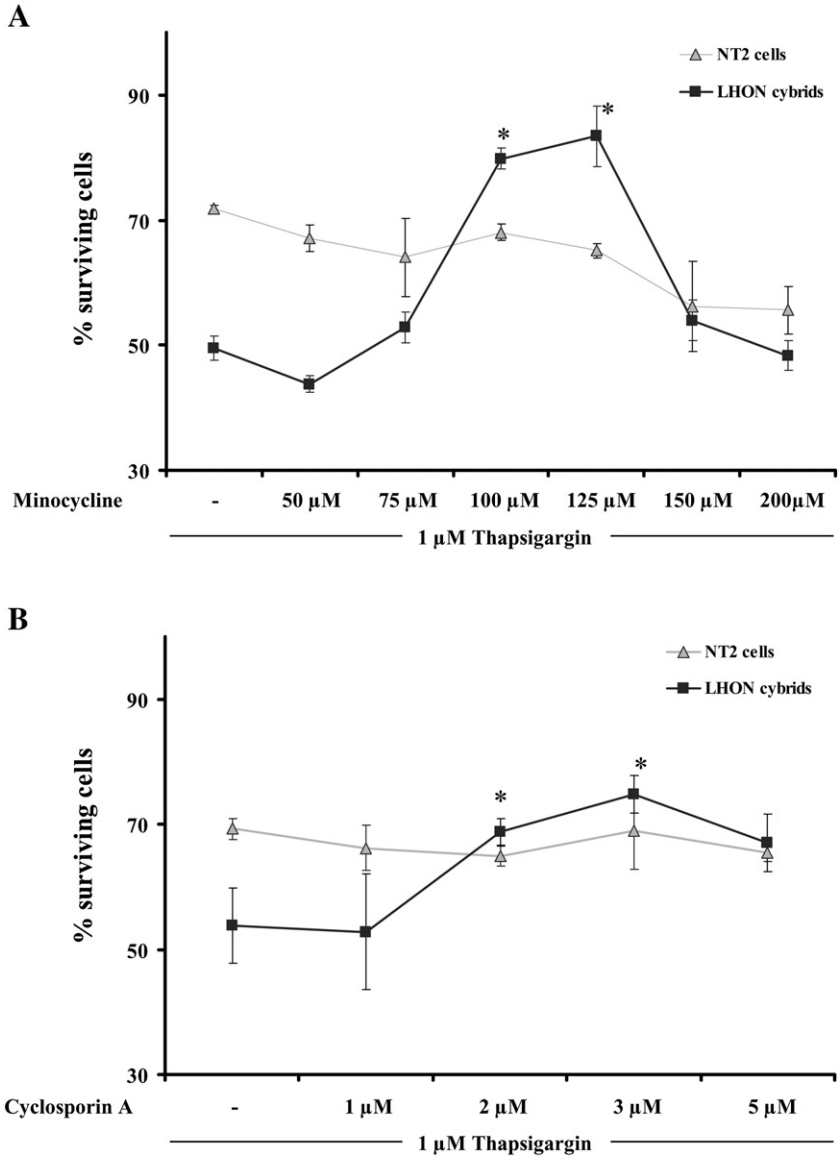

Fig. 1. LHON cybrid and NT2 cell survival assay and concentration response curve of minocycline (A) and CsA (B) against TG-induced cell death. The percentage of surviving cells compared to controls without TG treatment was calculated. (A) 100 μM minocycline was protective in the cybrid cells whereas in the parent cell lines it did not show protection at any concentration. Higher concentration did not show a significant improvement in the survival rate. On the contrary doses higher than 125 μM minocycline showed a toxic effect in the cybrid cells (*$p<0.01$). (B) In the parental cell line CsA did not provide protection but at a concentration of 2–3 μM was effective in the cybrid cells. 3 μM CsA resulted in a maximum survival in the cybrid cells (*$p<0.01$).

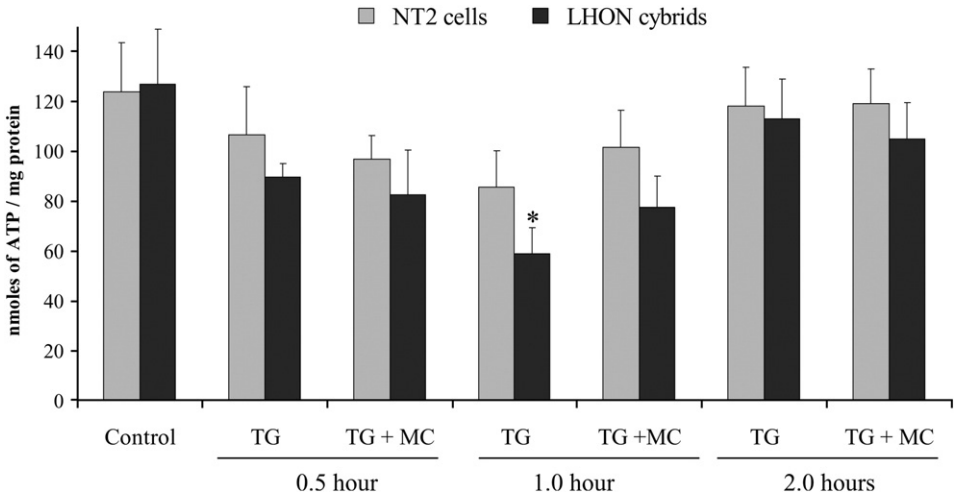

Fig. 2. ATP measurements in LHON cybrids and NT2 cells treated with 1 μM TG for 0.5, 1, or 2 h and with and without 100 μM minocycline (MC). A significant decline in ATP levels in the TG-treated LHON cybrids is seen at 1 h after the insult. The ATP levels significantly climbed back up at 2 h of TG treatment to a concentration insignificantly different to the normal untreated group (control). Minocycline does not have any significant effect on ATP levels of either LHON cybrids or NT2 cells in any group tested (*$p<0.05$).

NT2 cells did not show a significant decline after TG treatment in any of the measurements performed. We observed that minocycline insignificantly increased the ATP level after 1 h of TG treatment in LHON cybrids. However, minocycline treatment failed to significantly modify the ATP level changes brought by thapsigargin in both cell lines.

Minocycline and CsA alleviate Ca^{2+} deregulation

Cybrid cells in the Ca^{2+} imaging experiment (Fig. 3) exhibited a deregulation of cellular calcium upon TG perfusion after an initial stimulation with AcCh, which was indicated by a significantly higher sustained cytoplasmic level of calcium above the basal level (Fig. 3B). This sudden release and deregulation of calcium was alleviated in the LHON cybrids by 100 μM minocycline and 3 μM CsA (Fig. 3B). After the withdrawal of the excitatory stimulus, at 600 s of recording, the calcium fluorescent ratio values in minocycline (1.013±0.017; $n=5$) and CsA (1.03±0.005; $n=5$) treated groups significantly declined as compared to the AcCh/TG (1.069±0.004; $n=5$) per se group. This difference in fluorescent ratios of the respective treatments was maintained through the rest of the recordings. Two-way ANOVA (treatment × time) revealed that there was a significant difference between treatment groups ($F(3,112)=39.01$, $p<0.001$). In the NT2 cell line, however, no significant differences in the fluorescence values were observed and neither minocycline nor CsA alleviated the calcium deregulation induced by AcCh/TG at any time point after the withdrawal of the stimulus (Fig. 3C).

Mitochondrial membrane potential is conserved by minocycline

Results represented in Fig. 5 show that TG induced a significant decrease in the percentage of cells with active membrane potential in both cell lines (NT2 cells: 92.13±2.99%, $p<0.05$ and LHON cybrid: 68.54±4.93%, $p<0.01$). The degree of depolarization induced by thapsigargin in the two cell lines was also significantly different. The co-localization of TMRM and Mitotracker green, used as an indicator of functional mitochondria in proportion to the total population of mitochondria, was significantly increased in the minocycline (86.73±4.22%, $p<0.01$) as well as CsA (97.39%± 0.96, $p<0.01$) treated groups in LHON cybrid cells (Figs. 4 and 5A) ($F(2,104)=91.11$, $p<0.01$). However, neither minocycline (87.41±2.88%) nor CsA (90.56±2.98%) was effective in conserving the mitochondrial membrane potential loss in the NT2 cells treated with TG (Fig. 5B) ($F(2,59)=1.253$, $p=0.29$).

Active-caspase-3/procaspase-3 (aC3/pC3) ratio is decreased by minocycline and CsA

Western blots of LHON cybrid cells treated with TG ($n=5$) displayed an increase in the ratio of aC3/pC3 suggesting an activation of the downstream apoptotic event (Fig. 6). Quantification of the blots by densitometry exhibits a significant raise in the aC3/pC3 ratio in the LHON cybrid (2.82±0.19: $n=5$) treated with TG comparing to NT2 cells (1.78±0.15, $p<0.01$: $n=5$). One-way ANOVA showed a significant effect of treatments on the aC3/pC3 ratio in the cybrid cells ($F(3,26)=19.84$, $p<0.01$). A significant decrease in the ratio was seen in the LHON cybrid cells after minocycline (1.97±0.16: $n=5$) or CsA (1.35±0.23: $n=5$) treatments. In NT2 cells both minocycline (1.34±0.31: $n=4$) and CsA (1.1±0.38: $n=3$) failed to significantly decrease the TG-induced rise of the aC3/pC3 ratio.

Minocycline decreased the DFF fluorescence gain

Investigation of antioxidant properties of minocycline showed a significant dose dependent decrease in the DFF fluorescence by the drug (Fig. 7A). The basal level fluorescence in the LHON cybrids (35.94±3.13) declined significantly with 100 μM (18.86±4.18), 50 μM (22.43±1.38), and 25 μM (24.55±2.87) but not with 10 μM (26.59±4.10) minocycline (Fig. 7B), which suggests a dose dependent lowering in the oxidative stress level. The decreased basal fluorescence is comparable with the basal fluorescence observed in the NT2 cells (23.07±1.6). Vitamin C as an antioxidant also brings down the basal oxidative level in the cybrid cells (19.35±1.54; Fig. 7B). Subjecting the fluorescence

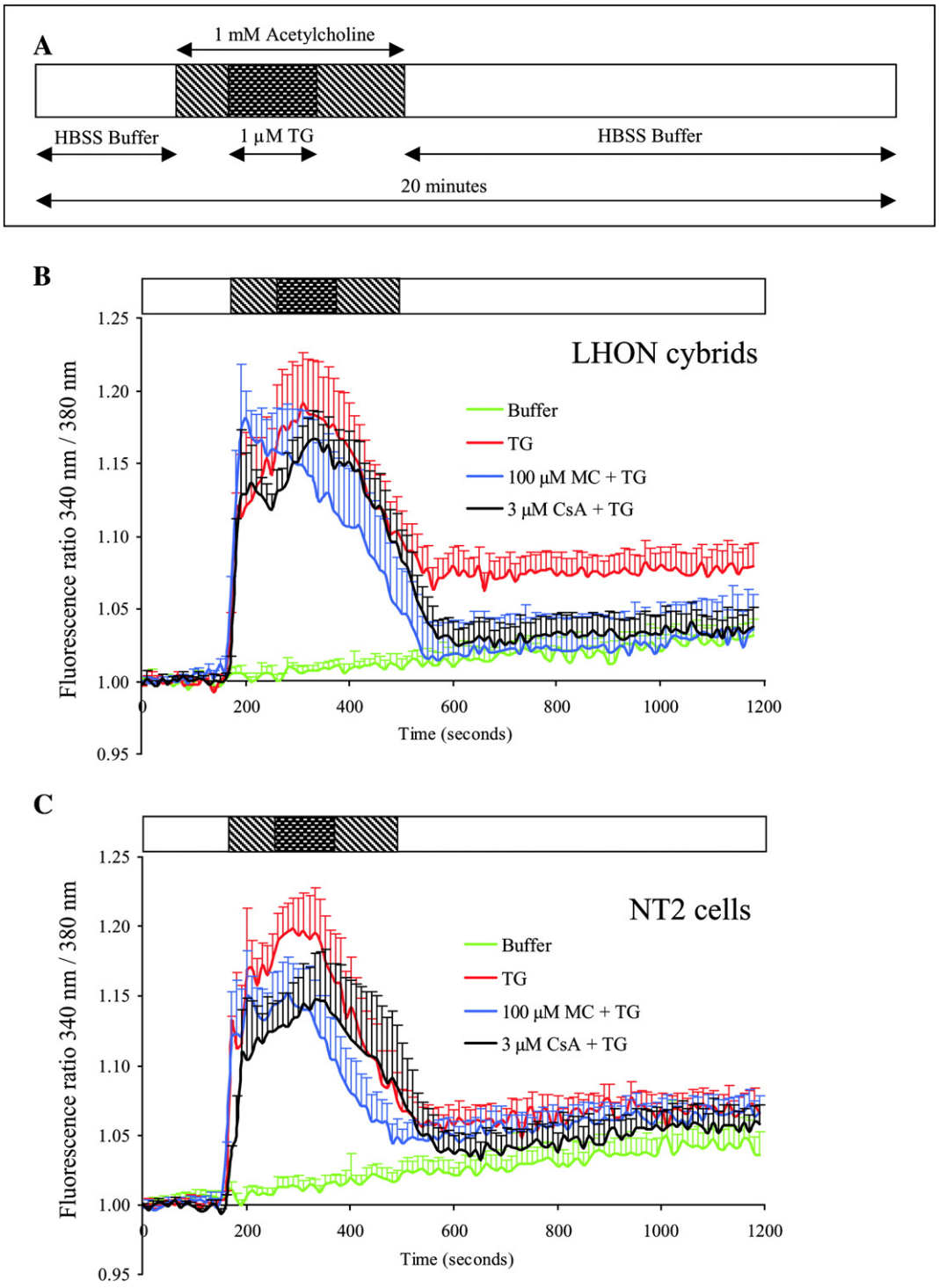

Fig. 3. Scheme of the cellular Ca^{2+} measurement experiments with live cell imaging is depicted in (A). The buffer is with or without 100 μM minocycline (MC) or 3 μM CsA, according to the experiment, throughout the perfusion. Acetylcholine is used initially to release calcium from the endoplasmic stores and TG to inhibit its reuptake. (B) Graph of the calcium imaging experiments with different treatments in LHON cybrid. Each experiment was repeated with five different batches of cultures, except for simple buffer (without AcCh/TG) perfusion that was repeated four times. A deregulation of the calcium signal induced by TG can be seen in the graph as the fluorescence does not drop to the baseline when the stimulus is withdrawn. Protective effect of 100 μM minocycline is evident by the drop of the calcium level to baseline after withdrawal of TG similar to that observed in CsA treatment. (C) Calcium deregulation induced by TG and the effect of minocycline and CsA in the NT2 cell line. The extent of calcium deregulation observed is lower than that produced in the LHON cybrids. Moreover minocycline and CsA could not significantly reduce the calcium deregulation by TG in the NT2 cell line.

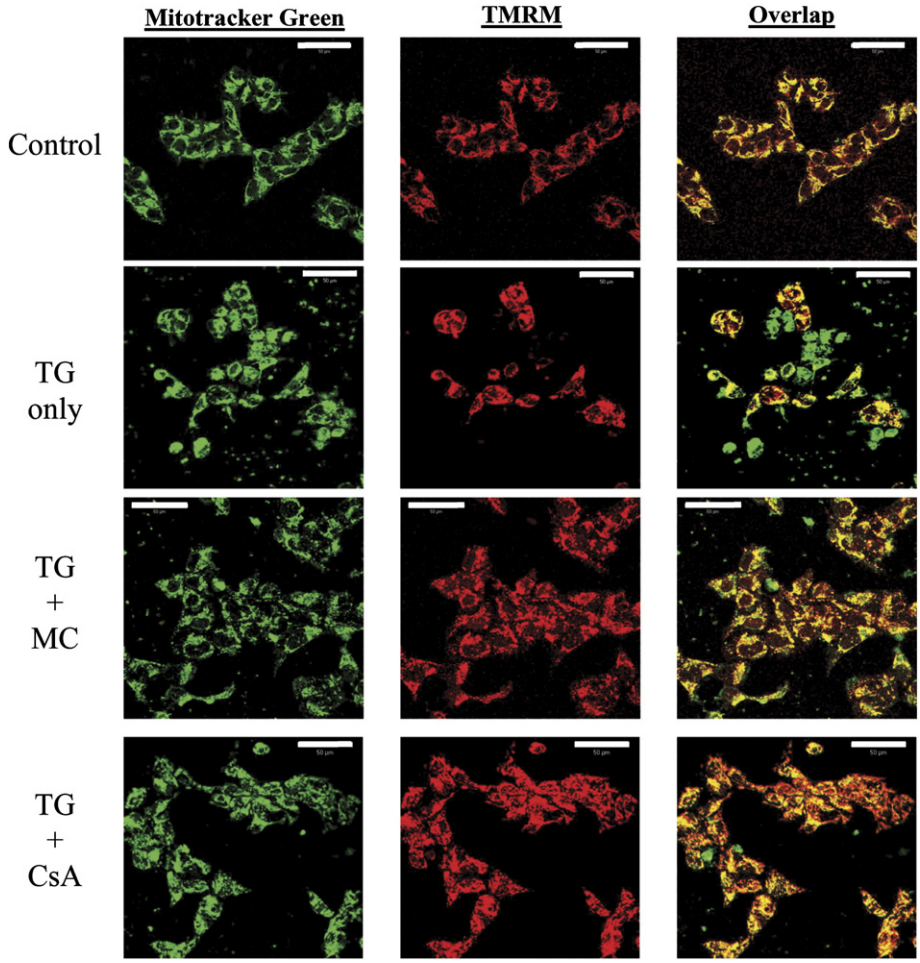

Fig. 4. Mitochondrial membrane potential imaging by TMRM uptake in LHON cybrid cells. Cells were incubated with TG (1 μM) for 8 h in serum-deprived medium. Mitotracker green is taken up by all mitochondria, whereas TMRM stains only those that have intact membrane potential. The conservation of $\Delta\Psi$ by minocycline (100 μM) and CsA (3 μM) is observed when compared to cultures that were treated with TG alone. Scale bars are 50 μm.

intensities of the first 100 s of imaging to one-way ANOVA between eight groups (NT2, LHON cybrids, LHON cybrids treated with four different minocycline concentrations, 3 μM CsA, and 100 μM vitamin C) reveals that the oxidative stress in the LHON cybrids was significantly lowered in both minocycline (25 μM, 50 μM, and 100 μM) and vitamin C treatments but not in the CsA (36.59±6.39) or lowest dose of minocycline (10 μM) treated groups ($F(7,49)=4.924$, $p<0.01$). A similar effect, as observed in the basal fluorescence intensities, was also seen after H_2O_2 injection (Fig. 8). Significant decrease in fluorescence intensities was detected with two of the higher but not the two lower doses of minocycline in comparison to the untreated group (Fig. 8A).

Discussion

The involvement of deregulation of cytosolic and intra-mitochondrial calcium in neurodegeneration has been shown by researchers to constitute a major mitochondrial pathway to apoptosis (Jacquard et al., 2006). The cause for the specific damage to the optic nerve was hypothesized by Beretta et al. showing that the glutamate uptake maximal velocity was significantly reduced in all LHON cybrid cell lines that correlated in a mutation-specific fashion with the degree of mitochondrial production of ROS (Beretta et al., 2004). They concluded that the retinal ganglionic cells in LHON disorder underwent excitotoxic damage induced by a defective glutamate transport leading to an insufficient withdrawal of retinal glutamate by Mueller cells. Under conditions of mitochondrial dysfunction ROS generation and the probability of mPTP opening increase, and both are directly related to mitochondrial Ca^{2+} accumulation (Brookes et al., 2004).

In our study TG, an irreversible smooth endoplasmic reticular calcium ATPase (SERCA) inhibitor (Lytton et al., 1991), along with acetylcholine (in our calcium imaging experiments used to cause an initial release of calcium), inhibits the reuptake of calcium to the endoplasmic stores and, thus, augments mitochondrial calcium accumulation (Hoek et al., 1997) to mimic neuronal overexcitation. Calcium being a positive effector of mitochondrial function stimulates respiratory pathways and leads to generation of ROS (especially in case of respiratory defects) creating an ideal condition for mPTP opening (Brookes et al., 2004).

The outcome of MTT cell survival assays (Fig. 1A) indicates that minocycline has a significant protective effect in the LHON cybrid cells at a concentration of 100 μM. Further increase in the concentration apparently does not lead to a more pronounced

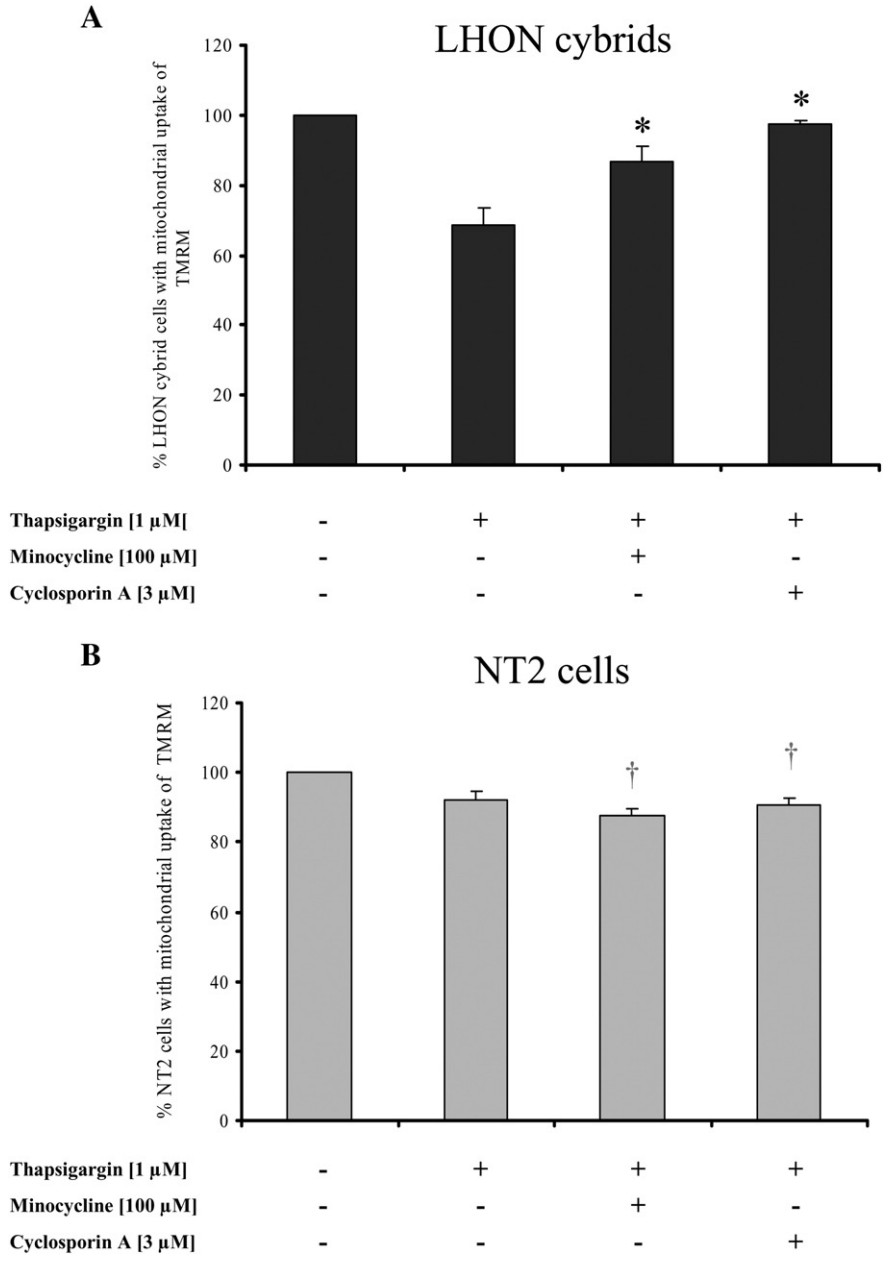

Fig. 5. Percentage of cells with preserved mitochondrial membrane potential with minocycline and CsA treatments after TG treatment in LHON cybrid cells and NT2 (parental cell line) as indicated by the uptake of TMRM. (A) A significant increase in the number of cells with preserved $\Delta\Psi$ was seen in the LHON cybrid cells with TG (1 μM) produced depolarization and with 100 μM minocycline or 3 μM CsA treatment (*$p<0.01$). (B) TG decreases the cell number with preserved $\Delta\Psi$ but no significant preservation of the same treatment with minocycline or CsA was seen in the NT2 cells (†$p>0.05$).

protection against TG-induced cell death. On the contrary we observed that higher concentrations of minocycline (150 and 200 μM) were toxic to the cells. In the parental NT2 cells minocycline was ineffective in providing protection against TG at any tested concentration. In our experiments, CsA was found to be comparatively effective in the cybrid cells at a concentration of 3 μM (Fig. 1B). This was also observed in the calcium imaging experiments where the deregulation of calcium was likewise alleviated. In the NT2 cells, however, none of the concentrations effective in the LHON cybrid cells was found to be protective as demonstrated by the survival rate of TG treated cells. This indicates that the mPTP may not play a role in decreasing the cell survival in the NT2 cells whereas it does in the LHON cybrid cells. The decrease in cell survival rate of NT2 cells by TG treatment can also be attributed at least partly to the ER stress response by depletion of the Ca^{2+} stores (Kitamura et al., 2003; Yoshida et al., 2006). This would also be true for the LHON cybrid cells. Furthermore, adding TG in combination with AcCh to the cells for a duration of 12 h did not differ from the TG-treated group per se in the MTT assay (data not shown). The decline of ATP level in LHON cybrids upon incubation with thapsigargin also points to calcium induced mitochondrial damage, a prerequisite for the induction of permeability transition leading to apoptosis (Brookes et al., 2004). Conservation of ATP (Fig. 2) may be necessary for

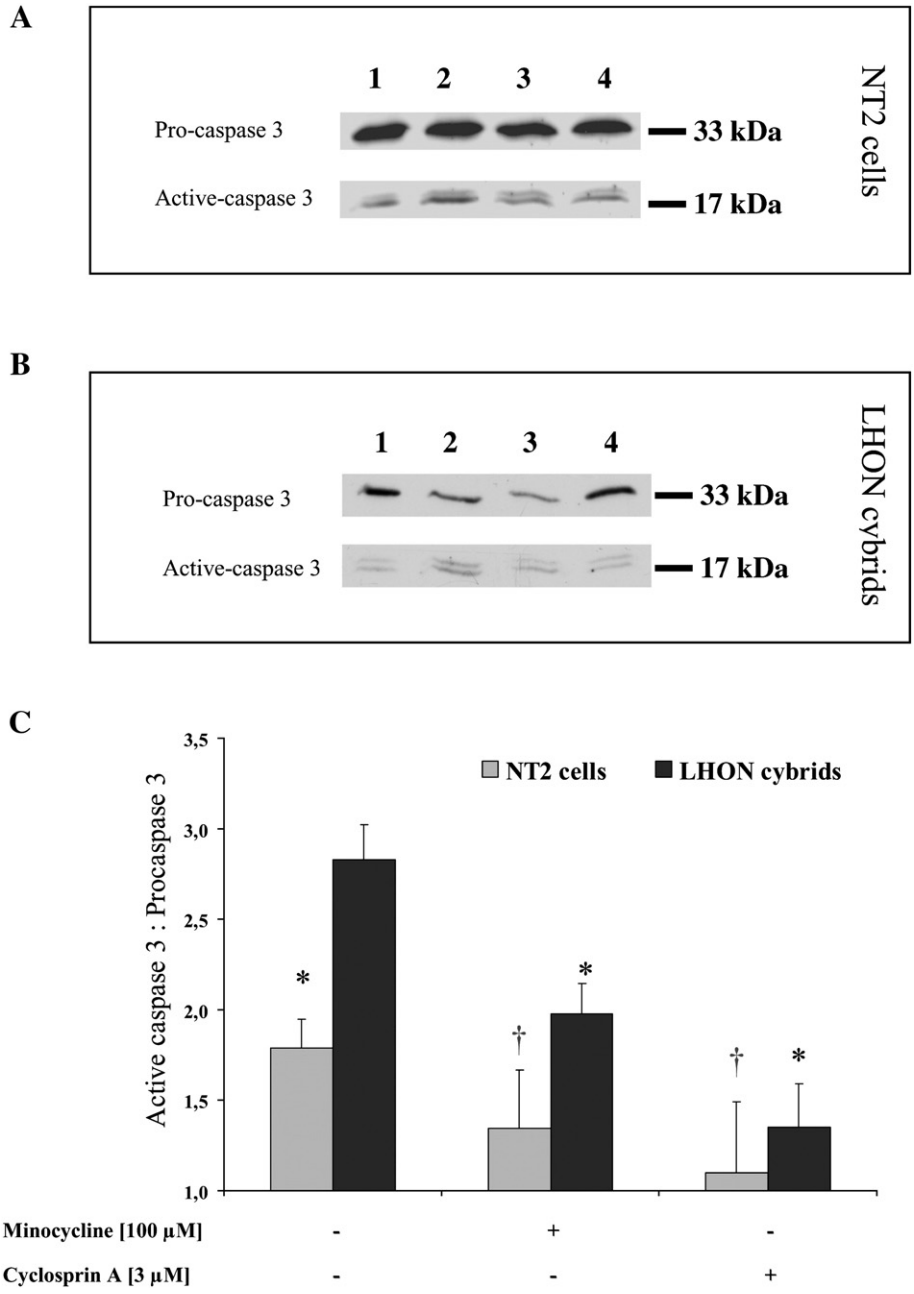

Fig. 6. Western blots of active-caspase-3 and procaspase-3 in NT2 (A) and LHON cybrid cells (B) following TG (1 µM) treatment for 8 h. Cells were additionally incubated with or without treatments (i.e. 100 µM minocycline or 3 µM CsA) in a serum free medium. Lane 1 = control (without TG), 2 = incubation with 1 µM TG, 3 = 1 µM TG + 100 µM minocycline, and 4 = 1 µM TG + 3 µM CsA. (C) Illustration of the aC3/pC3 ratio of different groups compared to the control (calculated as 1). CsA and minocycline significantly reduced the ratio in LHON cybrid cells but failed to significantly decrease that in the NT2 cell lines. Data are represented as arbitrary ratio units + S.E.M. *$p < 0.05$, †$p > 0.05$.

apoptosis to proceed. This recovery to normal ATP levels (per mg total protein) after 2 h may be explained by an adaptive up-regulation of the glycolytic pathway, if the cells are sensing energy failure. Cell death would not be avoided by this recovery of energy supply since mainly elicited by the mitochondrial apoptotic pathway (Zanna et al., 2005).

The participation of mPTP mediated apoptosis in cell death in the LHON cybrids is, however, strongly supported by the protective effect of CsA. In a situation where the reuptake of calcium back to the endoplasmic stores is inhibited by TG, mitochondria are expected to play the role of calcium buffering organelles that take up calcium from the cytoplasm, thereby increasing the matrix calcium (Ichas and Mazat, 1998; Korge and Weiss, 1999). This leads to a stimulation of the respiratory chain and increases free radical generation (especially in the case of respiratory chain mutations) and eventually results in the opening of the mPTP (Takeyama et al., 1993). This permeability transition leads to the release of mitochondrial calcium back into the cytosol. The normalization of calcium dynamics by mPTP inhibition has previously been discussed (Bernardi and Petronilli, 1996; Rizzuto

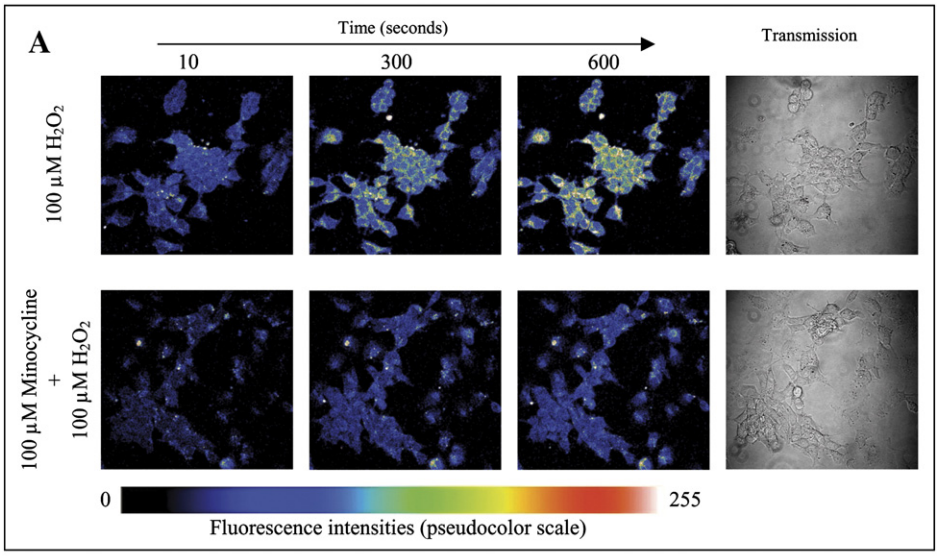

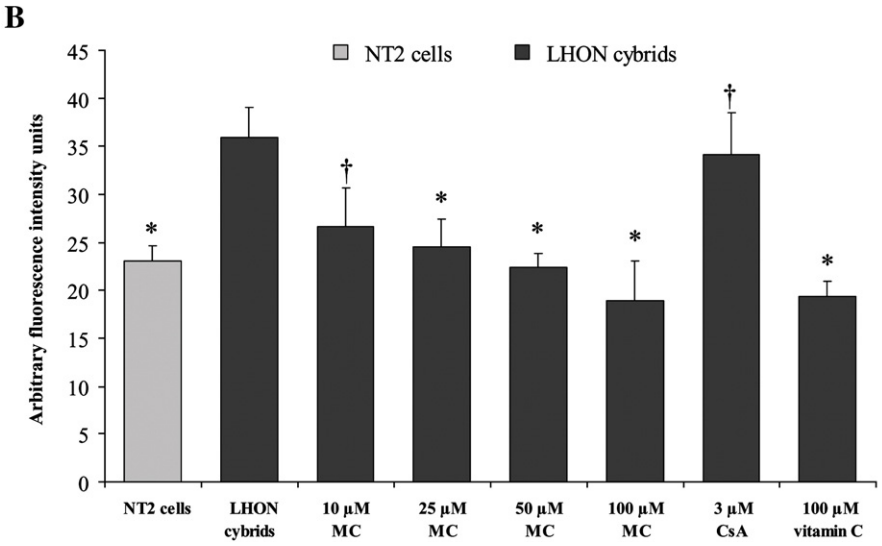

Fig. 7. DFF fluorescence live cell imaging of LHON cybrid cells. (A) Confocal images of LHON cybrid cells stimulated with 100 μM H_2O_2 with or without 100 μM minocycline (MC) treatment. The images are presented in gray scale intensities of 0–255. (B) Average initial fluorescence intensities of first 100 s of imaging (without H_2O_2) in different treatments. A significant decrease in the initial intensities in LHON cybrids is seen with both minocycline (25–100 μM) and vitamin C treatments but not with CsA and low concentration of minocycline (10 μM). *$p<0.05$, †$p>0.05$.

et al., 2000; Andrabi et al., 2004). In our live cell calcium imaging experiments minocycline had a similar pattern of effect on cellular calcium dynamics as CsA in AcCh/TG-induced deregulation of calcium in the cybrid cells. There are previous reports showing that minocycline is able, like CsA, to inhibit the permeability transition in isolated brain and liver mitochondria (Zhu et al., 2002; Fernandez-Gomez et al., 2005; Fuks et al., 2005). In contradiction Mansson et al. reported no direct inhibition of the mPTP by minocycline on isolated CNS mitochondria (Mansson et al., 2007).

As seen in our experiments the restoration of calcium dynamics suggests that in LHON cybrid cells minocycline is able to inhibit calcium overload-induced mPTP formation significantly. In the parental cell line, applying the same set of experiments, neither minocycline nor CsA showed any deviation of calcium dynamics from TG per se group as observed in the LHON cybrid cells. This indicates that the mPTP is not activated upon TG perfusion in the parental cell line. The increasing fluorescent ratio with buffer perfusion observed in cybrid cells and the parental cell line is most likely due to the leakage of the dye from the cells.

TMRM, a positively charged red fluorescent dye, is taken up by the mitochondria due to their negative membrane potential (Scaduto and Grotyohann, 1999). Upon opening of the mPTP the membrane potential of the mitochondria is lost (Blattner et al., 2001). Mitotracker green however is taken up by mitochondria irrespective of their membrane potential. The overlap of the two fluorescence images gives an idea of the proportion of cells that have intact mitochondrial membrane potential. TG has been earlier shown to decrease the mitochondrial membrane potential (Yamazaki et al., 2006). The presented data also suggest that TG decreases the number of cells with preserved mitochondrial membrane potential and that in

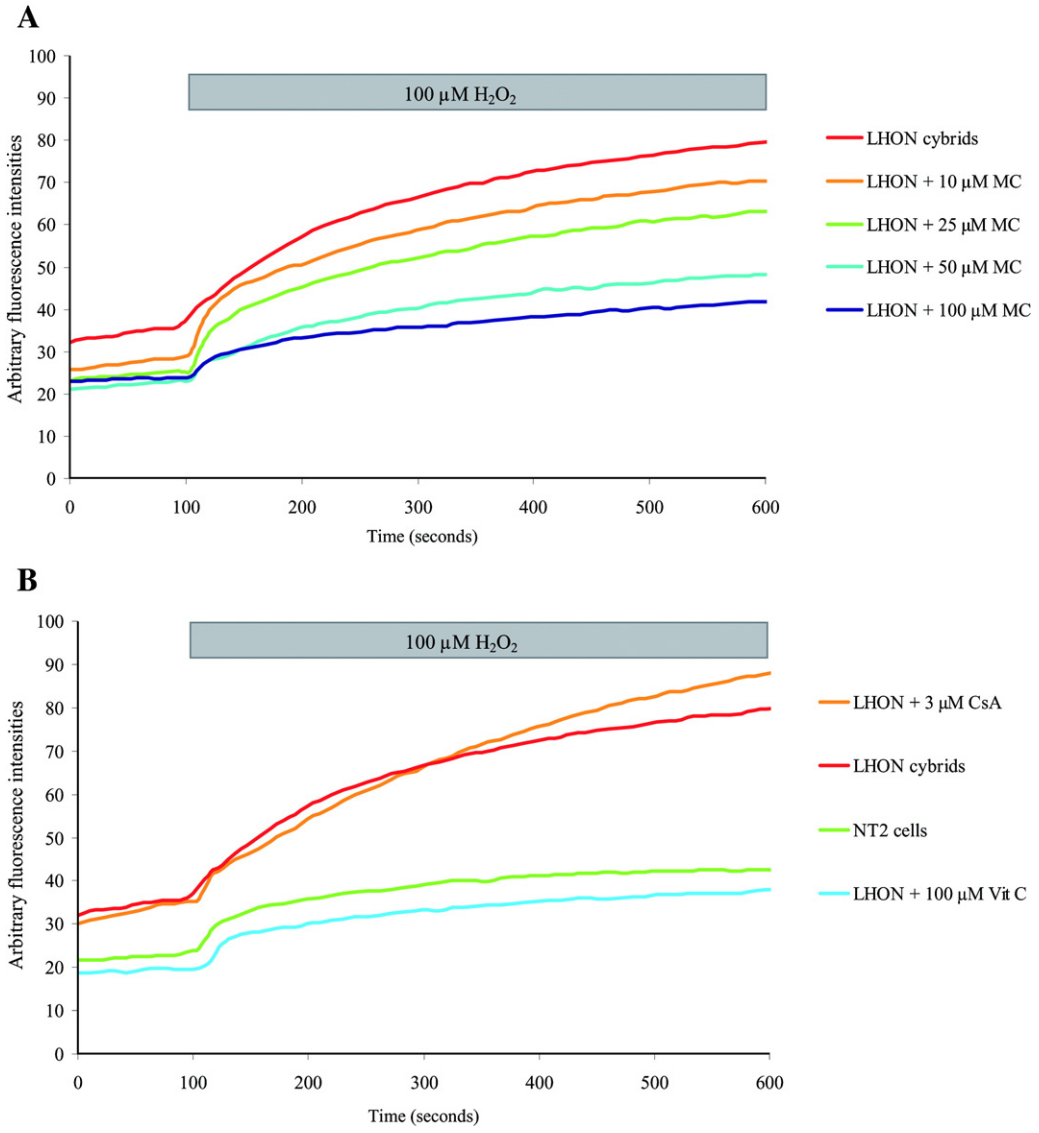

Fig. 8. Comparative graphs of DFF imaging with different treatments and stimulation with 100 μM H_2O_2 after 100 s. For clarity means without S.E.M. of at least 5 separated experiments are presented. (A) Comparison of DFF imaging fluorescence curve of NT2 cells with LHON cybrids without or with treatment (3 μM CsA or 100 μM vitamin C (Vit C)). (B) Dose dependent decrease in DFF fluorescence by minocycline treatment in LHON cybrids. Minocycline at all doses except the lowest significantly decreased the basal oxidative stress level similar to that observed with vitamin C suggestive of antioxidant property of minocycline. In addition the two higher concentration of minocycline (50 and 100 μM) decreased the fluorescence curves after H_2O_2 stimulus significantly, whereas the two lower concentrations did not.

cybrid cells minocycline can conserve the ΔΨ. The involvement of mPTP in this set of experiments is confirmed by the conservation of mitochondrial membrane potential by CsA, although CsA may also inhibit TMRM release from the cells by inhibiting multidrug resistance (MDR) related proteins, which may otherwise participate in ATP dependent TMRM outward transport through the plasma membrane. CsA has been recognized to be an inhibitor of such transport proteins (Wigler and Patterson, 1994). However, the minocycline effect is consistent with the one observed in our live calcium imaging experiments and suggests that minocycline could act as anti-apoptotic agent by inhibiting the mPTP *in vitro*. In NT2 cells even though the loss of mitochondrial membrane potential was significant in the TG-treated group, minocycline and CsA did not significantly reverse the dissipation of ΔΨ. This finding indicates that the mitochondrial membrane potential loss in the NT2 cells was CsA insensitive and therefore not due to mPTP. Western blot analysis reveals that the ratio of aC3/pC3 increases significantly more in the LHON cybrid cells than in the NT2 cells when treated with TG. This ratio is decreased by CsA treatment indicating that the permeability transition is involved, whereas the NT2 cells did not show a decrease in the ratio when treated with CsA. Minocycline also significantly decreased the ratio in the cybrid cells but not in the NT2 cells. This is in concurrence with the results of the cell viability assay in which both treatments showed no significant protection at the observed concentration and suggest that the mPTP is not activated under the present set of conditions in the parental cell line. It may not be surprising that the impact of CsA on cybrid survival, calcium response, membrane potential, and caspase-3 activation was even higher than that of minocycline because of the strong mPTP inhibitory action of CsA (Halestrap et al., 1997).

As mentioned in the Introduction section that the symptoms of LHON disorder are influenced by age, gender and environmental factors is commonly explained by a insufficient capacity of the cell to effectively deal with oxidative stress. With declining age the endogenous antioxidant pool and antioxidant enzyme activity of the cell decreases (Wei and Lee, 2002; Maher, 2005). In females the appearance of the LHON symptoms at a later age than in males can accordingly be explained by the presence of higher levels of estrogen, an upregulator of antioxidant genes (Vina et al., 2005). Smoking and alcohol consumption aggravate the oxidative load of the cell and consequently increase the relative risk of developing symptoms of LHON disorder (Tsao et al., 1999; Carelli et al., 2004). DFF imaging demonstrated a decrease in baseline fluorescence values with all except the lowest concentration of minocycline treatments similar to the decrease observed in vitamin C treatment suggestive of the antioxidant properties of the drug. On the other hand, the decrease was not observed with CsA as it lacks antioxidant properties. Induction of oxidative stress with H_2O_2 was dose dependently alleviated by minocycline as well as with 100 μM vitamin C but the same was not true for CsA treatment. These results support previous reports of antioxidant properties of minocycline (Kraus et al., 2005), which may contribute to its protective effect. Minocycline treatments reduced the basal fluorescence values and consequently the oxidative stress in LHON cybrids to a level where they are comparable to that observed in NT2 cells. Our findings suggest that minocycline, even at doses lower than 100 μM, can relieve the LHON cybrid cells of their inherent oxidative stress. The increase in cell viability seen in MTT assay was therefore not entirely dependent on the antioxidant property of the drug but also a consequence of mPTP pore inhibition similar to that revealed in our experiments by CsA treatment and in accordance with previous reports regarding minocycline being a megapore inhibitor (Zhu et al., 2002; Fernandez-Gomez et al., 2005; Fuks et al., 2005).

Therapies targeting the function of the respiratory chain (ETC) and targeting ETC born ROS species are currently under discussion. At present, a clinical trial with the antioxidative ubiquinone-analogue idebenone is performed in Great Britain, supervised by the Newcastle mitochondrial genetics group (Newcastle upon Tyne). In this trial, patients who developed recently LHON in one eye are experimentally treated with idebenone to rescue the second eye. Since individuals carrying a LHON mutation must not necessarily develop the disease, the risks of a general treatment of asymptomatic carriers are considered to be too high. It is well known, especially from investigations of the large Brazilian pedigree (Sadun et al., 2002, 2003, 2004), that even homoplasmic carriers must not necessarily develop the disease and that some additional risk factors, such as smoking, exist. Precise ophthalmologic investigations may help to identify carriers prone to develop LHON in the near future. While a general treatment of carriers is thus not indicated, the risk of applying the well-established drug minocycline in a "second eye approach" in humans might become tolerable, if some more data would have been collected in LHON models.

Although 2.0–3.0 μM CsA in our study well reversed partially the TG-induced toxicity the long term usage of such concentrations *in vivo* is certainly not applicable to human LHON disease. Blood concentrations in the target levels of 180–300 ng/ml (0.15–0.25 μM), occurring if CsA is used as an immunosuppressive drug, are known to cause several side effects in a percentage of patients. Besides increased arterial blood pressure, also several neurological complications have been described, such as tremor (in up to 40% of cases), mild encephalopathy (in up to 30%), seizures (1.5–6%), dysarthria, cerebellar ataxia, and peripheral neuropathy (for a review see Gijtenbeek et al., 1999). Thus *in vivo* the toxic side effects seem to exceed the desired protective effects, measurable in the cybrid system.

In contrast minocycline has a high safety profile and possess antioxidant properties, as demonstrated in our LHON model by DFF imaging. On the other hand, the achieved serum peak concentrations in humans are 6 μg/ml (around 12 μM) after 200 mg intravenous application (Saivin and Houin, 1988). It remains uncertain, whether sufficient tissue concentrations can be reached. In case of LHON, the blood–brain barrier has to be taken into account, which probably allows only small concentrations to reach the retinal ganglion cell layer and the optic nerve. However, recently Milane and colleagues performed blood–brain barrier transport studies in mice after intraperitoneal injection of 90 mg minocycline/kg and determined plasma concentrations of minocycline in the range of 40–60 μg/ml (around 80–120 μM) and corresponding brain/plasma ratio of around 0.08 (Milane et al., 2007). Similar results (2.8 μg/ml; approximately 6 μM) have been reported for cerebrospinal fluid from rats (Fagan et al., 2004). After oral administration (120 mg/kg) in mice after 8 h midbrain minocycline levels of 0.32 μg/g were described (Du et al., 2001). To our knowledge, no data are currently available concerning minocycline concentrations in retina or optic nerve. Theoretically, a direct application of minocycline into the vitreous may be taken into account, as it is already performed nowadays with e.g. anti-inflammatory drugs in some cases. However, this possibility seems to be rather unrealistic since even the acute phase of LHON must be viewed only as a manifestation of a basically chronic retinal disease, which would require a long term neuroprotective medication. The drug can be delivered efficiently only via oral or other systemic routes. The surprisingly small window of useful concentrations found in our cybrid experiments (100–150 μM) is in contrast to the broader therapeutic window observed during antibiotic therapy *in vivo*. This difference may just reflect the ineffective uptake of minocycline by our cybrid cells. Further studies are necessary to determine the local concentration needed around the optic nerve and to find out a relevant minocycline concentration in relation to a route of drug administration to reach neuroprotection *in vivo*. On the way to that point, it would be highly interesting to test the potential benefit of minocycline in a mouse LHON model, which was recently developed by the group of John Guy in Gainsville, USA (Qi et al., 2007). The authors showed for the first time that a transfection of mouse retina with viral vectors, allotopically expressing a mutant human ND4 subunit did develop elevated ROS production, optical nerve head swelling, apoptosis, and progressive loss of retinal ganglion cells. These effects did not occur in mice transfected with wild type human ND4. This is the first true genetic animal model of LHON, which should be suitable to test protective drug effects *in vivo* prior to a "second eye approach" in humans.

The lack of efficient uptake into the CNS and a probably narrow range of useful concentrations in the retinal ganglion cell layer may however limit the usefulness of minocycline in LHON therapy. Nevertheless, we conclude that the protective effect shown by minocycline in our experiments, along with its well-established clinical use, makes it an interesting drug for further investigations in therapy of LHON disease and possibly from other related disorders caused by mitochondrial respiratory chain defects.

Acknowledgments

We would like to thank Prof. Detlef Siemen for his valued discussions and expert advices. Technical assistance of Heike Baumann is greatly appreciated. This work was supported by funding provided by Magdeburger Forschungsverbund NBL3, project number BMBF 01ZZ0407.

References

Andrabi, S.A., Sayeed, I., Siemen, D., Wolf, G., Horn, T.F., 2004. Direct inhibition of the mitochondrial permeability transition pore: a possible mechanism responsible for anti-apoptotic effects of melatonin. FASEB J. 18, 869–871.

Baracca, A., Solaini, G., Sgarbi, G., Lenaz, G., Baruzzi, A., Schapira, A.H., Martinuzzi, A., Carelli, V., 2005. Severe impairment of complex I-driven adenosine triphosphate synthesis in Leber hereditary optic neuropathy cybrids. Arch. Neurol. 62, 730–736.

Beretta, S., Mattavelli, L., Sala, G., Tremolizzo, L., Schapira, A.H., Martinuzzi, A., Carelli, V., Ferrarese, C., 2004. Leber hereditary optic neuropathy mtDNA mutations disrupt glutamate transport in cybrid cell lines. Brain 127, 2183–2192.

Bernardi, P., Petronilli, V., 1996. The permeability transition pore as a mitochondrial calcium release channel: a critical appraisal. J. Bioenerg. Biomembr. 28, 131–138.

Blattner, J.R., He, L., Lemasters, J.J., 2001. Screening assays for the mitochondrial permeability transition using a fluorescence multiwell plate reader. Anal. Biochem. 295, 220–226.

Brookes, P.S., Yoon, Y., Robotham, J.L., Anders, M.W., Sheu, S.S., 2004. Calcium, ATP, and ROS: a mitochondrial love–hate triangle. Am. J. Physiol.: Cell Physiol. 287, C817–C833.

Brown, M.D., 1999. The enigmatic relationship between mitochondrial dysfunction and Leber's hereditary optic neuropathy. J. Neurol. Sci. 165, 1–5.

Carelli, V., Ghelli, A., Ratta, M., Bacchilega, E., Sangiorgi, S., Mancini, R., Leuzzi, V., Cortelli, P., Montagna, P., Lugaresi, E., Degli Esposti, M., 1997. Leber's hereditary optic neuropathy: biochemical effect of 11778/ND4 and 3460/ND1 mutations and correlation with the mitochondrial genotype. Neurology 48, 1623–1632.

Carelli, V., Ghelli, A., Bucchi, L., Montagna, P., De Negri, A., Leuzzi, V., Carducci, C., Lenaz, G., Lugaresi, E., Degli Esposti, M., 1999. Biochemical features of mtDNA 14484 (ND6/M64V) point mutation associated with Leber's hereditary optic neuropathy. Ann. Neurol. 45, 320–328.

Carelli, V., Ross-Cisneros, F.N., Sadun, A.A., 2004. Mitochondrial dysfunction as a cause of optic neuropathies. Prog. Retin. Eye Res. 23, 53–89.

Du, Y., Ma, Z., Lin, S., Dodel, R.C., Gao, F., Bales, K.R., Triarhou, L.C., Chernet, E., Perry, K.W., Nelson, D.L., Luecke, S., Phebus, L.A., Bymaster, F.P., Paul, S.M., 2001. Minocycline prevents nigrostriatal dopaminergic neurodegeneration in the MPTP model of Parkinson's disease. Proc. Natl. Acad. Sci. U. S. A. 98, 14669–14674.

Fagan, S.C., Edwards, D.J., Borlongan, C.V., Xu, L., Arora, A., Feuerstein, G., Hess, D.C., 2004. Optimal delivery of minocycline to the brain: implication for human studies of acute neuroprotection. Exp. Neurol. 186, 248–251.

Fehlings, M.G., Baptiste, D.C., 2005. Current status of clinical trials for acute spinal cord injury. Injury 36 (Suppl. 2), B113–B122.

Fernandez-Gomez, F.J., Galindo, M.F., Gomez-Lazaro, M., Gonzalez-Garcia, C., Cena, V., Aguirre, N., Jordan, J., 2005. Involvement of mitochondrial potential and calcium buffering capacity in minocycline cytoprotective actions. Neuroscience 133, 959–967.

Floreani, M., Napoli, E., Martinuzzi, A., Pantano, G., De Riva, V., Trevisan, R., Bisetto, E., Valente, L., Carelli, V., Dabbeni-Sala, F., 2005. Antioxidant defences in cybrids harboring mtDNA mutations associated with Leber's hereditary optic neuropathy. FEBS J. 272, 1124–1135.

Fuks, B., Talaga, P., Huart, C., Henichart, J.P., Bertrand, K., Grimee, R., Lorent, G., 2005. In vitro properties of 5-(benzylsulfonyl)-4-bromo-2-methyl-3(2*H*)-pyridazinone: a novel permeability transition pore inhibitor. Eur. J. Pharmacol. 519, 24–30.

Gijtenbeek, J.M., van den Bent, M.J., Vecht, C.J., 1999. Cyclosporine neurotoxicity: a review. J. Neurol. 246, 339–346.

Halestrap, A.P., Connern, C.P., Griffiths, E.J., Kerr, P.M., 1997. Cyclosporin A binding to mitochondrial cyclophilin inhibits the permeability transition pore and protects hearts from ischaemia/reperfusion injury. Mol. Cell. Biochem. 174, 167–172.

Head, E., Liu, J., Hagen, T.M., Muggenburg, B.A., Milgram, N.W., Ames, B.N., Cotman, C.W., 2002. Oxidative damage increases with age in a canine model of human brain aging. J. Neurochem. 82, 375–381.

Hoek, J.B., Walajtys-Rode, E., Wang, X., 1997. Hormonal stimulation, mitochondrial Ca2+ accumulation, and the control of the mitochondrial permeability transition in intact hepatocytes. Mol. Cell. Biochem. 174, 173–179.

Howell, N., 2003. LHON and other optic nerve atrophies: the mitochondrial connection. Dev. Ophthalmol. 37, 94–108.

Ichas, F., Mazat, J.P., 1998. From calcium signaling to cell death: two conformations for the mitochondrial permeability transition pore. Switching from low- to high-conductance state. Biochim. Biophys. Acta 1366, 33–50.

Jacquard, C., Trioulier, Y., Cosker, F., Escartin, C., Bizat, N., Hantraye, P., Cancela, J.M., Bonvento, G., Brouillet, E., 2006. Brain mitochondrial defects amplify intracellular [Ca2+] rise and neurodegeneration but not Ca2+ entry during NMDA receptor activation. FASEB J. 20, 1021–1023.

Jakubowski, W., Bartosz, G., 2000. 2,7-Dichlorofluorescin oxidation and reactive oxygen species: what does it measure? Cell Biol. Int. 24, 757–760.

Kantrow, S.P., Piantadosi, C.A., 1997. Release of cytochrome c from liver mitochondria during permeability transition. Biochem. Biophys. Res. Commun. 232, 669–671.

Kasapoglu, M., Ozben, T., 2001. Alterations of antioxidant enzymes and oxidative stress markers in aging. Exp. Gerontol. 36, 209–220.

Kim, J.M., Luo, L., Zirkin, B.R., 2000. Caspase-3 activation is required for Leydig cell apoptosis induced by ethane dimethanesulfonate. Endocrinology 141, 1846–1853.

Kitamura, Y., Miyamura, A., Takata, K., Inden, M., Tsuchiya, D., Nakamura, K., Taniguchi, T., 2003. Possible involvement of both endoplasmic reticulum- and mitochondria-dependent pathways in thapsigargin-induced apoptosis in human neuroblastoma SH-SY5Y cells. J. Pharmacol. Sci. 92, 228–236.

Korge, P., Weiss, J.N., 1999. Thapsigargin directly induces the mitochondrial permeability transition. Eur. J. Biochem. 265, 273–280.

Kraus, R.L., Pasieczny, R., Lariosa-Willingham, K., Turner, M.S., Jiang, A., Trauger, J.W., 2005. Antioxidant properties of minocycline: neuroprotection in an oxidative stress assay and direct radical-scavenging activity. J. Neurochem. 94, 819–827.

Lytton, J., Westlin, M., Hanley, M.R., 1991. Thapsigargin inhibits the sarcoplasmic or endoplasmic reticulum Ca-ATPase family of calcium pumps. J. Biol. Chem. 266, 17067–17071.

Maher, P., 2005. The effects of stress and aging on glutathione metabolism. Ageing Res. Rev. 4, 288–314.

Mansson, R., Hansson, M.J., Morota, S., Uchino, H., Ekdahl, C.T., Elmer, E., 2007. Re-evaluation of mitochondrial permeability transition as a primary neuroprotective target of minocycline. Neurobiol. Dis. 25, 198–205.

Milane, A., Fernandez, C., Bensimon, G., Meininger, V., Farinotti, R., 2007. Simple liquid chromatographic determination of minocycline in brain and plasma. Chromatographia 65, 277–281.

Qi, X., Sun, L., Lewin, A.S., Hauswirth, W.W., Guy, J., 2007. The mutant human ND4 subunit of complex I induces optic neuropathy in the mouse. Invest. Ophthalmol. Visual Sci. 48, 1–10.

Rizzuto, R., Bernardi, P., Pozzan, T., 2000. Mitochondria as all-round players of the calcium game. J. Physiol. 529 (Pt. 1), 37–47.

Sadun, A.A., Carelli, V., Salomao, S.R., Berezovsky, A., Quiros, P., Sadun, F., DeNegri, A.M., Andrade, R., Schein, S., Belfort, R., 2002. A very large Brazilian pedigree with 11778 Leber's hereditary optic neuropathy. Trans. Am. Ophthalmol. Soc. 100, 169–178.

Sadun, A.A., Carelli, V., Salomao, S.R., Berezovsky, A., Quiros, P.A., Sadun, F., DeNegri, A.M., Andrade, R., Moraes, M., Passos, A., Kjaer, P., Pereira, J., Valentino, M.L., Schein, S., Belfort, R., 2003. Extensive investigation of a large Brazilian pedigree of 11778/haplogroup J Leber hereditary optic neuropathy. Am. J. Ophthalmol. 136, 231–238.

Sadun, F., De Negri, A.M., Carelli, V., Salomao, S.R., Berezovsky, A., Andrade, R., Moraes, M., Passos, A., Belfort, R., da Rosa, A.B., Quiros, P., Sadun, A.A., 2004. Ophthalmologic findings in a large pedigree of 11778/Haplogroup J Leber hereditary optic neuropathy. Am. J. Ophthalmol. 137, 271–277.

Saivin, S., Houin, G., 1988. Clinical pharmacokinetics of doxycycline and minocycline. Clin. Pharmacokinet. 15, 355–366.

Scaduto Jr., R.C., Grotyohann, L.W., 1999. Measurement of mitochondrial membrane potential using fluorescent rhodamine derivatives. Biophys. J. 76, 469–477.

Schauser, K., Larsson, L.I., 2005. Programmed cell death and cell extrusion in rat duodenum: a study of expression and activation of caspase-3 in relation to C-jun phosphorylation, DNA fragmentation and apoptotic morphology. Histochem. Cell Biol. 124, 237–243.

Schoeler, S., Winkler-Stuck, K., Szibor, R., Haroon, M.F., Gellerich, F.N., Chamaon, K., Mawrin, C., Kirches, E., 2007. Glutathione depletion in antioxidant defense of differentiated NT2-LHON cybrids. Neurobiol. Dis. 25, 536–544.

Takeyama, N., Matsuo, N., Tanaka, T., 1993. Oxidative damage to mitochondria is mediated by the Ca(2+)-dependent inner-membrane permeability transition. Biochem. J. 294 (Pt. 3), 719–725.

Tsao, K., Aitken, P.A., Johns, D.R., 1999. Smoking as an aetiological factor in a pedigree with Leber's hereditary optic neuropathy. Br. J. Ophthalmol. 83, 577–581.

Vina, J., Borras, C., Gambini, J., Sastre, J., Pallardo, F.V., 2005. Why females live longer than males? Importance of the upregulation of longevity-associated genes by oestrogenic compounds. FEBS Lett. 579, 2541–2545.

Wei, Y.H., Lee, H.C., 2002. Oxidative stress, mitochondrial DNA mutation, and impairment of antioxidant enzymes in aging. Exp. Biol. Med. (Maywood) 227, 671–682.

Wigler, P.W., Patterson, F.K., 1994. Reversal agent inhibition of the multidrug resistance pump in human leukemic lymphoblasts. Biochim. Biophys. Acta 1189, 1–6.

Wong, A., Cavelier, L., Collins-Schramm, H.E., Seldin, M.F., McGrogan, M., Savontaus, M.L., Cortopassi, G.A., 2002. Differentiation-specific effects of LHON mutations introduced into neuronal NT2 cells. Hum. Mol. Genet. 11, 431–438.

Yamazaki, T., Muramoto, M., Oe, T., Morikawa, N., Okitsu, O., Nagashima, T., Nishimura, S., Katayama, Y., Kita, Y., 2006. Diclofenac, a non-steroidal anti-inflammatory drug, suppresses apoptosis induced by endoplasmic reticulum stresses by inhibiting caspase signaling. Neuropharmacology 50, 558–567.

Yong, V.W., Wells, J., Giuliani, F., Casha, S., Power, C., Metz, L.M., 2004. The promise of minocycline in neurology. Lancet Neurol. 3, 744–751.

Yoshida, I., Monji, A., Tashiro, K., Nakamura, K., Inoue, R., Kanba, S., 2006. Depletion of intracellular Ca2+ store itself may be a major factor in thapsigargin-induced ER stress and apoptosis in PC12 cells. Neurochem. Int. 48, 696–702.

Zanna, C., Ghelli, A., Porcelli, A.M., Martinuzzi, A., Carelli, V., Rugolo, M., 2005. Caspase-independent death of Leber's hereditary optic neuropathy cybrids is driven by energetic failure and mediated by AIF and Endonuclease G. Apoptosis 10, 997–1007.

Zhu, S., Stavrovskaya, I.G., Drozda, M., Kim, B.Y., Ona, V., Li, M., Sarang, S., Liu, A.S., Hartley, D.M., Wudu, C., Gullans, S., Ferrante, R.J., Przedborski, S., Kristal, B.S., Friedlander, R.M., 2002. Minocycline inhibits cytochrome c release and delays progression of amyotrophic lateral sclerosis in mice. Nature 417, 74–78.